RSC Sustainability

ROYAL SOCIETY OF CHEMISTRY

PAPER

View Article Online
View Journal | View Issue

Cite this: *RSC Sustainability*, 2024, **2**, 528

Mechanochemical Cu(II) complexes and propargylamine synthetic adventures†

Ghadah Abdullah S. Al Jomeh,[a] Andrew McGown,[a] Emma Richards,[b] Graham J. Tizzard,[c] Simon J. Coles,[c] Ramón González-Méndez,[a] Chris Dadswell,[a] John Spencer[a] and George E. Kostakis[*a]

Received 7th September 2023
Accepted 8th January 2024

DOI: 10.1039/d3su00315a

rsc.li/rscsus

We synthesized and characterized known and new Cu(II)–salen complexes and investigated their efficacy in yielding propargylamines (PAs) *via* an A^3 coupling reaction mechanochemically. Although the method appears simple, we explicitly describe synthetic obstacles that urge unavoidable solvent use to isolate the molecular entities in high purity. The recovered complexes retain structure and catalytic efficacy, and a library of twenty-four known and unknown PAs are isolated in very good to excellent yields. The scope and limitations of this method are presented.

Sustainability spotlight

The present portable methodology can be used in any developing country, escapes from traditional catalytic methods, and uses minimal solvent and abundant elements to produce heterobifunctional molecules that could remove specific unwanted proteins. This method aligns with UN SDG(s) 3, 9 and 12 and explicitly with targets 3.4, 9.4, 12.1 and 12.5.

Introduction

Traditional chemical processes often use toxic reagents and fossil fuels and generate harmful byproducts, significantly contributing to environmental pollution.[1,2] Alternative, sustainable methods have been sought in the last two decades to minimize waste, decrease or avoid toxic materials, and incorporate renewable resources.[3–5] Mechanochemistry uses mechanical forces, such as grinding or milling, to initiate or drive chemical reactions rather than relying on traditional solvent-based methods.[6–11] Work by Toda *et al.* evidenced the reproducibility of several organic reactions, occurring in solution, in the solid state by mixing the ingredients into finely powdered form.[12,13] Ball-milling represents a sophisticated upgrade of traditional grinding, minimizes waste, reduces energy consumption and can be easily scaled up for industrial production and thus can be considered a sustainable synthetic method, although its applicability can be limited in terms of capital expense (equipment costs), efficiency, and selectivity.[8]

Propargylamines (PAs) are valuable precursors for organic scaffolds used for neurodegenerative diseases or as anti-depressants, anti-platelets and anticonvulsants.[14,15] They can be synthesized *via* traditional catalytic protocols, based on alkylation or reductive amination paths, that incorporate Pd-based or Zn alkynyl reagents or sodium borohydride in significant amounts.[16] The A^3 coupling reaction is a popular organic pathway for synthesizing PAs in the presence of late (Cu, Pd, or Au) transition metals.[17–29] This process involves three substrates, amine–alkyne–aldehyde and the *in situ* formation of a π complex (metal-alkyne), which weakens the C–H sp bond with subsequent proton elimination by a weak base, resulting in σ activation and formation of the acetylide, which can be subsequently added to the imine (product of the amine–aldehyde condensation), yielding the PA.[14] The A^3 coupling reaction has been a desirable target for mechanochemical synthesis, as it allows for the rapid and efficient construction of complex molecules with high structural diversity. In 2015, Su *et al.* demonstrated a solvent-free enantioselective PAs synthesis *via* a $Cu(OTf)_2$/Ph-pybox system by ball-milling within 60 minutes. The *in situ* generated catalytic system can be reused several times without losing activity and applies to a broad scope of substrates, aromatic aldehydes and amines.[23] In 2018, the mechanochemical activation of aldehydes, amines, and calcium carbide in the presence of CuI enabled the unprecedented formation of 1,4-diamino-2-butynes under solventless conditions.[30]

[a]*Department of Chemistry, School of Life Sciences, University of Sussex, Brighton BN1 9QJ, UK. E-mail: G.Kostakis@sussex.ac.uk*

[b]*School of Chemistry, Cardiff University, Main Building, Park Place, Cardiff CF10 3AT, Wales, UK*

[c]*UK National Crystallography Service, Chemistry, University of Southampton, SO1 71BJ, UK*

† Electronic supplementary information (ESI) available: ^{1}H-NMR, ^{13}C-NMR, HRMS, TG, IR, EPR, UV-Vis, CD. CCDC 2284741–2284750. For ESI and crystallographic data in CIF or other electronic format see DOI: https://doi.org/10.1039/d3su00315a

Our group have investigated the peculiar efficiency of Cu(II) complexes as vehicles to promote the A^3 coupling reaction, in the absence of additives, at low loadings and in non-coordinating solvents.[31,32] We identified the unprecedented efficacy of the neutral Cu(II)–N_2O_2 salen complex (Scheme 1), facilitating the A^3 coupling at room temperature within 72 h.[31] The reaction proceeds *via* a radical pathway, and the (N or O) heteroatoms of the salen frame act as a weak base to eliminate the proton from the alkyne while the reaction rate increases with temperature. The recovered complex retains its structure and catalytic efficacy after 10 cycles. The complex can be synthesized in two simple high-yielding steps from commercially available starting materials. The first step involves a condensation reaction, reflux for three hours, of the parent diamine and the 3,5-di-*tert*-butyl salicylaldehyde in MeOH, while the second step involves the complexation reaction of the resulting Schiff base and $Cu(OTf)_2$. Inspired by the aforementioned solventless A^3 reports and given the synthetic simplicity of these two steps, we envisioned the solventless ligand, Cu(II)–N_2O_2 salen complex, and PAs synthesis as feasible. To the best of our knowledge, a few studies have already reported the solventless synthesis of salen based complexes in one-pot[33] or two steps,[34–37] but no report identifies the synthesis of the ligand, complex and PAs mechanochemically. The results of this effort and the scope and limitations of this approach are described herein.

Results

Ligand synthesis

The solventless ligand synthesis, as anticipated, is a straightforward procedure. Initial screenings, varying the frequency and the milling time, identified the optimum conditions (Table 1, entry 6). A detailed optimisation table can be found in the ESI (Table S1†). The ligand purity was identified by ^{1}H and ^{13}C NMR, IR, and ESI-MS, although two important observations should be considered for future reference. Using steel-based balls and jars and/or prolonged reactions (40 or 80 minutes) yielded yellow solids for which the ^{1}H NMR identified the presence of a different species (results not shown in Table 1), possibly the ketonic form of the targeted species, in a 4 : 1 ratio (Fig. S1 and S2†). The presence of additional peaks in the aromatic and aliphatic regions and integration comparison could support this observation and the *tert*-butyl groups act as convenient fingerprints in identifying a 4 : 1 ratio. Moreover, the IR data (Fig. S3†) of the yellow solids indicate the absence of the hydroxyl group and H-bonding interactions (3500–3000 cm^{-1}) and the presence of a ketone (C=O) bond at 1700 cm^{-1}. In contrast, the use of Teflon-based jars and ceramic balls eliminates the formation of the other species. After overcoming these obstacles, we could successfully synthesise the chiral versions (Table 1, entries 7 and 8, H_2**L1**). All ligands were characterised by ^{1}H and ^{13}C NMR, IR, UV-Vis, ESI-MS, while their chiral nature was confirmed by circular dichroism (Fig. S4 and S5†). Thereafter, we extended the study to a different chiral diamine (Table 1, entries 9 and 10, H_2**L2**). As before, we performed several reactions; the use of a steel-based jar and balls for 80 minutes yielded a mixture of diol–ketone forms in a 4 : 1 ratio, as previously, thus supporting our choice to use only Teflon based jars and balls (see ^{1}H NMR data Fig. S6†). Single crystal X-ray diffraction studies of a recrystallised material from MeOH for the prolonged experiment identified loss of chirality (Table S1 and Fig. S7†); a notion that should be considered for future investigations for us and others. However, when the reactions are performed for a short period (*i.e.* 10 minutes) with Teflon and ceramic components, chirality is retained. The single-crystal X-ray diffraction results are similar to the recently reported components (Table S2†).[38,39] As for the first family of ligands, *SS*-H_2**L2** and *RR*-H_2**L2** were characterised by ^{1}H and ^{13}C NMR, IR, UV-Vis, ESI-MS, while their chirality was determined by circular dichroism (Fig. S4†). After reaction completion, the solids were placed in the oven (60 °C) overnight to dry. This process is convenient compared with reactions performed in the presence of molecular sieves, which eliminates water molecules as byproducts, but requires treatment with solvent to obtain the targeted species.

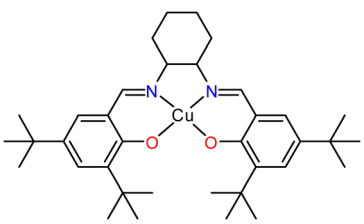

Scheme 1 A schematic representation of the Cu(II)–N_2O_2 salen complex used in previous studies.[31]

Complex synthesis

With the ligands in hand, we then focused on the synthesis of the corresponding complexes. The crystalline complex made under reflux conditions with lack of lattice solvent molecules and decomposition starting at 282 °C was used as the benchmark, and we employed thermogravimetric analysis (TGA) as a tool to identify impurities and to determine the optimal reaction conditions (Fig. 1).[31] We screened several parameters, altering (a) slightly the metal salt : ligand ratio (0.95 : 1, 1 : 1, 1 : 1.05); (b) the metal salt, incorporating weakly (Cl, Br, OTf, BF_4) or strongly coordinating (NO_3, OAc) anions; (c) the frequency; and (d) the time of the reaction (Table S3†). Also, we incorporated the ligand(s) with(out) drying overnight, ligand(s) made under reflux solvent conditions. The optimal conditions were determined to be as follows: ceramic balls, Teflon-based jars, metal salt : ligand ratio 1 : 1, $CuCl_2$ as the Cu(II) source, 180 minutes and ball-milling frequency 25 Hz.

We chose $CuCl_2$ as the metal salt because it bears a weakly coordinating anion and no lattice solvent molecules. The reaction of the ligand *racemic*-H_2**L1**, without drying, with $CuCl_2$ in 1 : 1 molar ratio resulted in a brownish material possessing a significant amount of lattice molecules (at 138 °C presents 20% weight loss). It is worth noting that two hydrochloric acid molecules (Scheme 2) are produced during the complexation reaction.

Table 1 Ball mill synthesis conditions of the ligands reported in this work. Data shown were obtained using ceramic balls and Teflon-based jars

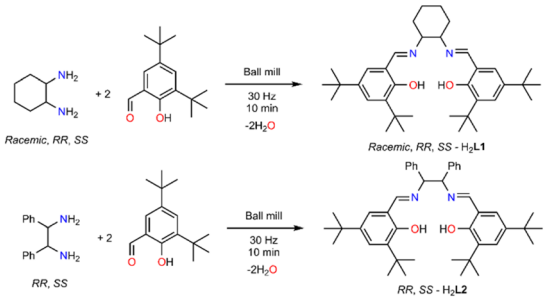

Entry	Amine–aldehyde ratio	Time (min)	Frequency (Hz)	Yield (%)	Ligand
1	1 : 2	5	3	—	*Racemic*-H_2**L1**
2	1 : 2	5	5	—	*Racemic*-H_2**L1**
3	1 : 2	5	10	—	*Racemic*-H_2**L1**
4	1 : 2	5	15	50	*Racemic*-H_2**L1**
5	1 : 2	5	20	70	*Racemic*-H_2**L1**
6	1 : 2	10	25	>99	*Racemic*-H_2**L1**
7	1 : 2	10	25	>99	*RR*-H_2**L1**
8	1 : 2	10	25	>99	*SS*-H_2**L1**
9	1 : 2	10	25	>99	*RR*-H_2**L2**
10	1 : 2	10	25	>99	*SS*-H_2**L2**

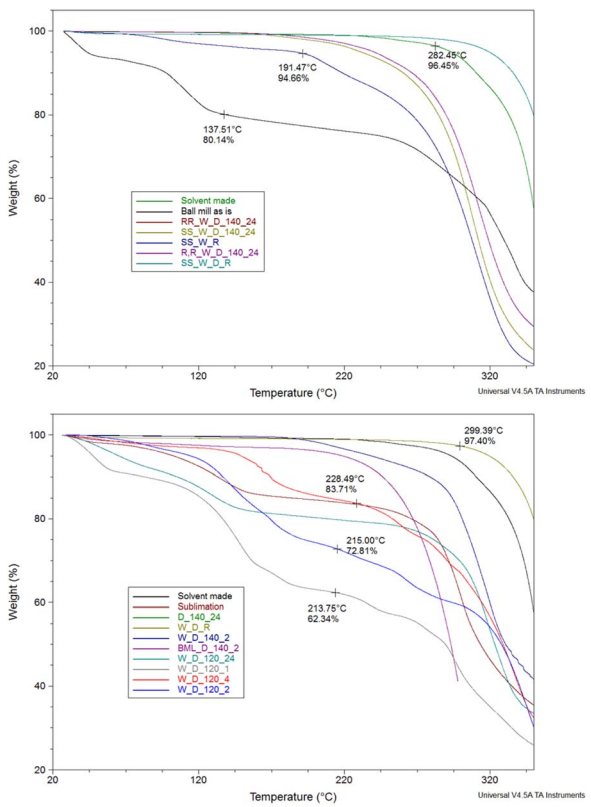

Fig. 1 Thermogravimetric analysis of different trials; washed (W), dried (D), recrystallised (R) drying temperatures (120 or 140 °C), drying time (1, 2, 4 or 24 hours), chiral versions (*RR*/*SS*).

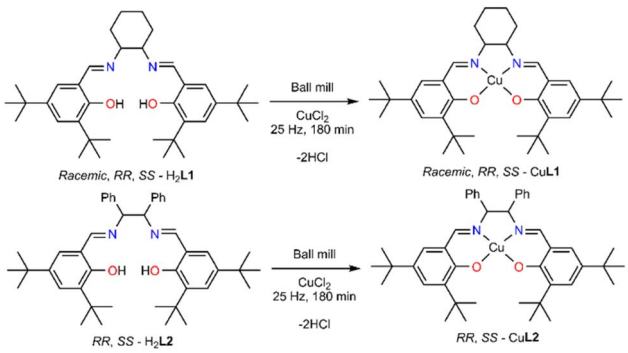

Scheme 2 Solventless synthesis of Cu**L1** and Cu**L2**.

Given this notion, we washed the final product with five drops (~0.25 ml) of water to remove hydrochloric acid and dried it for different times (1, 2, 24 h) or temperatures (120 or 140 °C), aiming to identify the least energy consuming conditions. However, none of these efforts delivered a solid product with similar thermal behaviour to the benchmark material. Next, we attempted to sublime the produced material, but again we obtained material containing a significant amount of lattice molecules. After all these trials, we identified that recrystallisation from a minimal amount of non-coordinating and volatile acetone provides a solid with identical thermal behaviour to the parent molecule. PXRD studies of the products, in bulk, strongly deviate from the calculated pattern, possibly indicating crystallisation in a different space group (Fig. S8†). Last, we adopted the previously described one-pot synthesis,[33] (Table S3,† entry 28); however, the yield of the targeted material was

only 30% after washing, drying and recrystallisation. After optimising this process, we applied this synthetic protocol to obtain all the Cu(II) complexes; the yield for all five complexes is over 99%. The synthesis of the final molecules in the solid state was further validated by recording elemental analysis and supplementary EPR studies. The EPR spectrum of solid dehydrated *SS*-Cu**L2** is shown in Fig. S13,† indicating an approximately pseudo-axial profile but with no resolvable copper hyperfine splitting, as would be expected for the spin active metal centre $I(^{63,65}\mathrm{Cu}) = 3/2$. Further weak signals at half-field ($B \sim 150$ mT) are typical of high-spin (*i.e.* $S > \frac{1}{2}$) spin systems and suggests magnetic interaction between neighbouring metal centres in the solid state (Table S5†). Therefore, for improved resolution of the spin Hamiltonian parameters characterizing the paramagnetic centre, further measurements were performed in a toluene : dichloromethane solvent system in the presence of the A^3 substrates (Fig. S13–S18†). *SS*-Cu**L2** is characterized by a predominantly axial **g**-tensor ($g_{\|} = 2.150$, $g_{\perp} = 2.010$; $g_{iso} = 2.056$) and dominated by copper hyperfine coupling ($A_{\|} = 590$, $A_{\perp} = 90$ MHz; $a_{iso} = 256.7$ MHz), in which the **g**-tensor and **A**-tensor are coincident with the molecular frame, as reported previously for a closely analogous derivative of Cu**L1** in which the cyclohexyl backbone is replaced by a phenyl ring.[40] The spin Hamiltonian parameters characterizing the EPR spectra change upon addition of the A^3 coupling components, notably an increase in the $g_{\|}$ value accompanied by a decrease in $A_{\|}$ (Fig. S13–S18†), indicating transfer of electron spin density away from the copper centre through weak coordination of the substrate to an axial coordination site. This is analogous to previous reports for binding of chiral amines to Schiff-base complexes.[41,42]

To determine the absolute structure of the resulting complexes, we recorded single crystal X-ray diffraction data for compounds *SS*-Cu**L2** and *RR*-Cu**L2** (Table S2†), and identified the unit cell data (data not presented) for compounds *SS*-Cu**L1**, *RR*-Cu**L1** and *racemic*-Cu**L1**.[43] For compounds *SS*-Cu**L2** and *RR*-Cu**L2** (Fig. 2 and Table S4†), the structures are solved in chiral space groups, in contrast to the already known data.[44] To our surprise, one of the screening reactions with steel-based jars and balls, *RR*-H_2**L2** and $CuCl_2$, yielded a crystalline byproduct material formulated as *RR*-FeCl**L2** (Fig. 2, bottom) that was not further characterised but intimated that metal leaching from either the jar or balls could occur during the milling process. All these studies identify the technical obstacles in our efforts to obtain the targeted complexes in high purity, despite the simplicity of the system and previous reports for one or two-step procedures.[33–37] Furthermore, the produced complexes are susceptible to absorbing moisture from the environment as determined by elemental analysis (ESI†); therefore, the final complexes should be stored in the oven at 60 °C or be "activated" before use in any catalytic reaction. All these factors are essential when applying these chiral complexes in the asymmetric A^3 coupling reactions or for redox purposes.[45] In solution, the complexes retain their chiral character (Fig S9†), and showcase a typical UV-Vis spectrum corresponding to a tetradentate N_2O_2 chromophore (Fig S10†), while the ESI-MS data provide structures of the absolute formulae (Fig S11 and S12†).

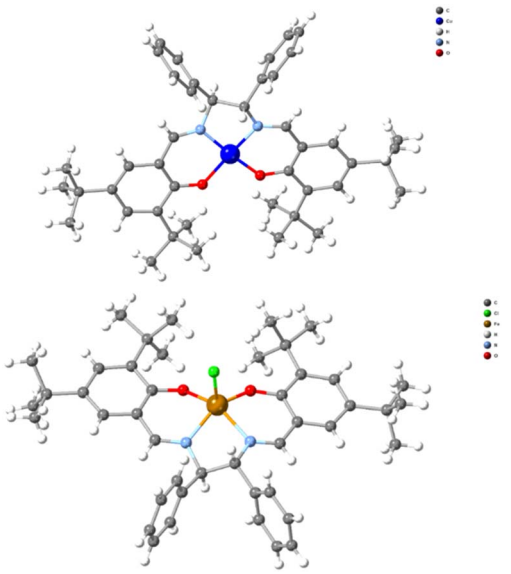

Fig. 2 A projection of compound *SS*-Cu**L2** and the unprecedented byproduct (*RR*-FeCl**L2**) was observed when steel-based jars and balls were used.

Propargylamine synthesis

We aimed to identify the optimum conditions for the A^3 coupling reaction with the high-purity complexes in our hands.[23,30] As previously, we chose cyclohexanecarboxaldehyde, pyrrolidine, and phenylacetylene as model substrates to evaluate the title reaction,[31] and incorporated the *racemic*-Cu**L1** as the catalyst. Table 2 and Fig. 3 provide the average yield and calculated standard deviation out of at least three trials. Our first control experiments focused on determining the impact of the type of jar and/or number of balls; however, a reaction using Teflon-based jars and balls failed to produce the desired product (Table 2, entry 1 and Fig S19†). Given that reactions with steel-based jars led to the production of unwanted (*RR*-FeCl**L2**) impurities *vide supra*, we discarded their use for catalytic reactions. Hence, we instead attempted the reaction using already known conditions,[23,30] or modified jars and balls and the substrate molar ratio to optimise our protocol (Table 2, entries 2–9). The reaction in the presence of silica gel[23] does not improve performance (entry 3, Table 2). We identified that the optimum substrate ratio is cyclohexanecarboxaldehyde (1.5 mmol), pyrrolidine (1.5 mmol), and phenylacetylene (1 mmol).

Using molecular sieves to capture the *in situ* generated water molecules improves performance (entry 10, Table 2); however, incorporation of the drying agents complicates the recovery process, requiring additional solvent treatment, thus we decided to proceed without their use. These salen complexes are susceptible to absorbing moisture upon storage, which significantly impacts performance (entry 9, Table 2), although storing the complex at 60 °C or activation prior to catalysis is required for optimum performance (entry 11, Table 2). To our delight,

Table 2 Control experiments to identify the optimum conditions for the A^3 coupling reaction

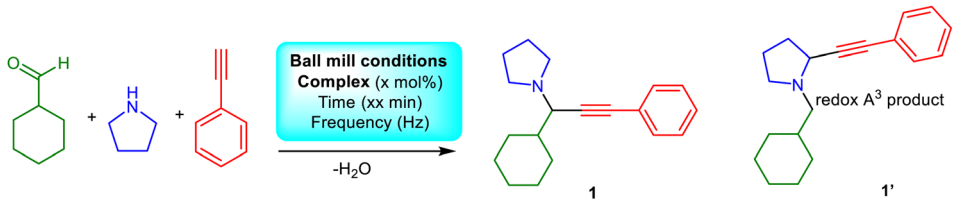

Entry	Aldehyde (mmol)	Amine (mmol)	Alkyne (mmol)	Cu source (% mol)	Time (h)	Frequency (Hz)	Conversion[a] (%)
1	1.5	1.5	2	—	3	25	NR[b]
2	1.2	1.1	1	*rac*-Cu**L1** (**5**)	2	25	32
3	1.0	1.2	1.5	*rac*-Cu**L1** (**7**)	2	25	NR[c]
4	1	1.1	1.2	*rac*-Cu**L1** (**2**)	2	25	34[d]
5	1	1.1	1.2	*rac*-Cu**L1** (**5**)	3	25	52[e]
6	1	1.1	1.2	*rac*-Cu**L1** (**5**)	3	25	59[f]
7	1.5	1.5	1.0	*rac*-Cu**L1** (**5**)	3	25	81[g]
8	1.5	1.5	1.0	*rac*-Cu**L1** (**5**)	3	25	89[h]
9	1.5	1.5	1.0	*rac*-Cu**L1** (**2**)	3	25	92 (**3**)[h]
10	1.5	1.5	1.0	*rac*-Cu**L1** (**2**)	3	25	99 (**3**)[h,i]
11	1.5	1.5	1.0	*rac*-Cu**L1** (**2**)	3	25	99 (**1**)[h,j]
12	1.5	1.5	1.0	$CuCl_2$ (**2**)	3	25	NR[h]
13	1.5	1.5	1.0	$CuCl_2$ (**10**)	3	25	NR[h]
14	1.5	1.5	1.0	$CuCl_2$ (**20**)	3	25	90 (**1**)/9 (**1′**)[h]
15	1.5	1.5	1.0	$CuCl_2$ (**2**) + H_2**L1** (**2**)	3	25	NR[h]
16	1.5	1.5	1.0	$CuCl_2$ (**20**) + H_2**L1** (**20**)	3	25	90 (**1**)/9 (**1′**)[h]
17	1.5	1.5	1.0	*rac*-Cu**L1** (**2**)	3	25	93 (**3**)[h,k]
18	1.5	1.5	1.0	*rac*-Cu**L1** (**2**)	3	25	99 (**1**)[h,j,l]
19	1.5	1.5	1.0	*rac*-Cu**L1**[m]	3	25	20[h]
20	1.5	1.5	1.0	*rac*-Cu**L1**[n]	3	25	31[h]
21	1.5	1.5	1.0	*SS*-Cu**L1**	3	25	99 (**1**)[h,j]
22	1.5	1.5	1.0	*RR*-Cu**L1**	3	25	99 (**1**)[h,j]
23	1.5	1.5	1.0	*SS*-Cu**L2**	3	25	99 (**1**)[h,j]
24	1.5	1.5	1.0	*RR*-Cu**L2**	3	25	99 (**1**)[h,j]

[a] Calculated conversion from crude ^{1}H NMR. Number in parenthesis represents standard deviation while those in bold represent formation of different product. [b] NR symbolises no reaction. [c] Silica gel present. [d] Stainless steel jar & stainless steel ball. [e] Stainless steel jar & ceramic ball. [f] Plastic jar & ceramic ball. [g] Stainless steel jar & ceramic ball. [h] Plastic jar & ceramic ball. [i] In the presence of molecular sieves. [j] Complex stored in the oven (60 °C). [k] Recovered. [l] Recovered dried (10th time). [m] We used complex named "*Ball mill as is*" (Fig. 1, left). [n] We used complex named "*W_D_120_1*" (Fig. 1, right).

the reaction employing the same substrate ratio of $CuCl_2$ instead of the *racemic*-Cu**L1** complex, does not promote the A^3 coupling. Higher copper salt loadings (10%, 20%) yield the anticipated product and its redox analogue (entries 12–14, Table 2, Fig. S20 and S21†), which, according to the literature, corresponds to the redox A^3 coupling product.[46,47] Our efforts to *in situ* generate the complex from $CuCl_2$ and *racemic*-H_2**L1** in loadings 2% and 20% either did not yield the expected product (entry 15, Table 2), or yielded the expected compounds in addition to the byproduct **1′** (entry 16, Table 2), signifying the importance of isolating the well-characterised complexes prior to catalysis.

Treating the reaction with isopropanol,[31] allows for recovery of the complex and single crystal X-ray diffraction studies (Table S4†) and catalytic trials of the recovered material identify that it retains its structure and catalytic efficacy after ten cycles (entries 17 and 18, Table 2). Also, we tested the catalytic efficacy of the "impure" complexes (entries 19 and 20, Table 2), and, to our delight, identified moderate performance, justifying our persistence and choice to use well-characterised complexes. After optimising the conditions, we expanded our study to the other complexes, which outperformed the others (entries 21–24, Table 2). Finally, we attempted to expand the scope of the method to other substrates (Fig. 3). The method applies to aliphatic aldehydes, secondary amines, and various alkynes and provides twenty PAs in very good to excellent yields, demonstrating the excellent utility of this approach.

To further expand and understand the limitations of our method, and given the chiral nature of the PA products, we attempted enantioselective determination for compound **1** (entries 21–24, Table 2). To our disappointment, analysis with a chiral column identified the formation of only racemic products (Fig. S22–S26†). Then, to evaluate copper metal leaching during the process, we performed a series of ICP-MS studies with(out) the use of a metal scavenger and the results are shown in Table 3. These data suggest that the amount of Cu found in the synthesised PAs using *racemic*-Cu**L1** is significantly below the acceptable limits with or without using a metal

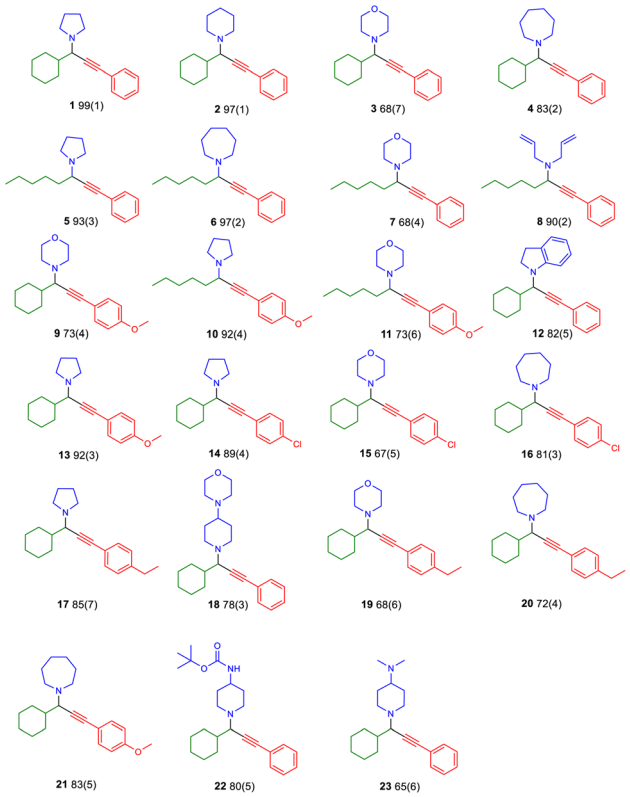

Fig. 3 Substrate scope of the reaction with aldehydes, secondary amines and alkynes. Isolated yields, after purification. Reaction conditions; catalyst (2 mol%), 1.5 mmol aldehyde, 1.5 mmol amine, 1.0 mmol alkyne, time 3 h, frequency 25 Hz. Numbers in parenthesis represent the standard deviation ($n = 3$).

scavenger, which confirms that metal leaching from the active catalyst does not occur during the catalytic process.[48] A comparison with a reaction using 20% $CuCl_2$ loading (reactions with 2% or 10% loading do not proceed) suggests that using a metal scavenger is vital, greatly reducing the remaining Cu entity in the organic scaffold.

Lastly, to evaluate the applicability of our method and given the very good yield in isolating PA **22**, we expanded our study to the synthesis of PA **24**.

The chosen PA can be used as a template for synthesising heterobifunctional molecules. Compound **24** can be synthesised under microwave irradiation on a gram scale (method A; Scheme 3), however, using our protocol, **24** can be synthesized up to 500 mg scale (method B).

Discussion

Building on our previous studies,[31] this work investigated the solventless synthesis of Cu(II) salen complexes and propargylamines. Despite the simplicity of the task, we identified significant synthetic technical obstacles and the unavoidable use of a minimum amount of solvent to access the complexes in high purity. This notion is vital considering, for example, similar molecular scaffolds used in the electrochemical CO_2 reduction and formation of C^{2+} products;[45] the presence of impurities may affect catalytic performance significantly, as is the case in this study.

The Cu(II) complexes catalyse the A^3 coupling reaction yielding twenty-four PAs in very good to excellent yields, but most importantly, the recovered molecular complexes retain their structure and catalytic efficacy after ten reaction cycles. Control experiments applaud the use of well-characterised species over metal salts that retain structure and efficacy and are hence recoverable, requiring one order of magnitude less loading and resulting in Cu content (as impurities) within the final organic species that are significantly below the acceptable limits. The method reported herein (ligand, complex and PA synthesis) uses significantly less solvent than our previous study, proceeds to completion in a shorter period (Table 4), incorporates non-toxic, abundant, commercially available chemicals, and operates

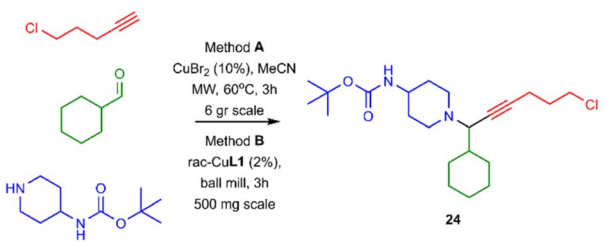

Scheme 3 The application of our protocol and gram-scale synthesis of organic scaffold **24**.

Table 3 Data for comparison purposes of the remaining Cu amounts post catalysis

Entry	Catalyst (loading%)	Metal scavenger	Yield (%)	ICP-MS Cu detection level (ppm)
1	*rac*-Cu**L1** (**2**)	Yes	99 (**1**)	0.25
2	*rac*-Cu**L1** (**2**)	No	99 (**1**)	0.43
3	*rac*-Cu**L1** (**10**)	Yes	99 (**1**)	0.61
4	*rac*-Cu**L1** (**10**)	No	99 (**1**)	3.31
5	$CuCl_2$ (**2**)	Yes	No reaction	—
6	$CuCl_2$ (**2**)	No	No reaction	—
7	$CuCl_2$ (**10**)	Yes	No reaction	—
8	$CuCl_2$ (**10**)	No	No reaction	—
9	$CuCl_2$ (**20**)	Yes	90 (**1**)/9 (**1′**)	0.01
10	$CuCl_2$ (**20**)	No	90 (**1**)/9 (**1′**)	0.23

Table 4 Summary of complex and A^3 coupling catalysis protocol for current and previous work

	Previous work[31]			This work		
	Solvent	Time	Yield (%)	Solvent	Time	Yield (%)
Ligand synthesis	EtOH	2 h	97	None	15 min	>99
Complex synthesis	MeOH	1 h	90	None	15 min	>99
Complex purification	Not needed			Acetone/water		
Complex recovery post catalysis	Isopropanol			Isopropanol		
PAs synthesis	DCM	72 h	97	None	3 h	>99
PAs purification	EtOAc/hexane			EtOAc/hexane		

in the open air. It therefore, has a significant "green" character and is sustainable compared to traditional catalytic methods.

Conclusions

We encountered several synthetic/technical obstacles in our effort to transition from traditional catalytic protocols to greener methodologies and provide functional organic scaffolds conveniently. We entrust the reported exemplary method paves the way for modern and sustainable coordination and synthetic principles and will be inspirational for several research groups.

Author contributions

GEK devised the project with critical input from GAJ. GAJ synthesised and characterised the ligands and complexes, performed the catalytic studies and purified the propargylamines. GAJ recorded the thermogravimetric analysis data. GAJ, GEK, GJT, SJC produced and processed crystallographic data. ER recorded the EPR data. RGM performed MS studies. CD performed ICP-MS studies. AM and JS assisted in the method optimisation and purification of organic products. All authors contributed to the preparation of the article.

Conflicts of interest

There are no conflicts to declare.

Acknowledgements

GAJ thanks Imam Muhammed Ibn Saud University for offering financial support for a PhD fellowship. GEK thanks the EPSRC UK National Crystallography Service at the University of Southampton for collecting the crystallographic data.[49] GEK/ER acknowledge financial support from RSC Research Enablement Grant (E22-9127990267). AM, GEK, JS are grateful to the University of Sussex for HEIF Business Collaboration & Commercialisation 2023 funding. We thank Prof. Louise C. Serpell and Dr Youssra Al-Hilaly (Sussex Neuroscience) for accessing the Circular Dichroism apparatus. We acknowledge REACH Separations Ltd in Biocity Nottingham for chirality determination of the products.

References

1 P. T. Anastas, *Crit. Rev. Anal. Chem.*, 2010, **29**, 167–175.
2 P. Anastas and N. Eghbali, *Chem. Soc. Rev.*, 2010, **39**, 301–312.
3 C. J. Elsevier, J. Reedijk, P. H. Walton and M. D. Ward, *Dalton Trans.*, 2003, 1869–1880.
4 A. Reichle and O. Reiser, *Chem. Sci.*, 2023, **14**, 4449–4462.
5 M. C. Leech and K. Lam, *Nat. Rev. Chem.*, 2022, **6**, 275–286.
6 J. Yu, X. Yang, C. Wu and W. Su, *J. Org. Chem.*, 2020, **85**, 1009–1021.
7 A. Porcheddu, E. Colacino, L. De Luca and F. Delogu, *ACS Catal.*, 2020, **10**, 8344–8394.
8 S. Hwang, S. Grätz and L. Borchardt, *Chem. Commun.*, 2022, **58**, 1661–1671.
9 T. Friščić, C. Mottillo and H. M. Titi, *Angew. Chem., Int. Ed.*, 2020, **59**, 1018–1029.
10 O. Galant, G. Cerfeda, A. S. McCalmont, S. L. James, A. Porcheddu, F. Delogu, D. E. Crawford, E. Colacino and S. Spatari, *ACS Sustain. Chem. Eng.*, 2022, **10**, 1430–1439.
11 S. L. James and T. Frišcic, *Chem. Soc. Rev.*, 2013, **42**, 7494–7496.
12 F. Toda, K. Tanaka and S. Iwata, *J. Org. Chem.*, 1989, **54**, 3007–3009.
13 K. Tanaka and F. Toda, *Chem. Rev.*, 2000, **100**, 1025–1074.
14 J. Farhi, I. N. Lykakis and G. E. Kostakis, *Catalysts*, 2022, **12**, 660.
15 K. Lauder, A. Toscani, N. Scalacci and D. Castagnolo, *Chem. Rev.*, 2017, **117**, 14091–14200.
16 A. Kumar, P. Sharma, N. Sharma, Y. Kumar and D. Mahajan, *RSC Adv.*, 2021, **11**, 25777–25787.
17 B. V. Rokade, J. Barker and P. J. Guiry, *Chem. Soc. Rev.*, 2019, **48**, 4766–4790.
18 V. A. Peshkov, O. P. Pereshivko, A. A. Nechaev, A. A. Peshkov and E. V. Van der Eycken, *Chem. Soc. Rev.*, 2018, **47**, 3861–3898.
19 G. Abbiati and E. Rossi, *Beilstein J. Org. Chem.*, 2014, **10**, 481–513.
20 S. Shah, B. G. Das and V. K. Singh, *Tetrahedron*, 2021, **93**, 132238.
21 Q. Liu, H. Xu, Y. Li, Y. Yao, X. Zhang, Y. Guo and S. Ma, *Nat. Commun.*, 2021, **12**, 1–10.
22 C. Koradin, K. Polborn and P. Knochel, *Angew. Chem., Int. Ed.*, 2002, **41**, 2535–2538.
23 Z. Li, Z. Jiang and W. Su, *Green Chem.*, 2015, **17**, 2330–2334.

24 C. Wetzel, P. C. Kunz, I. Thiel and B. Spingler, *Inorg. Chem.*, 2011, **50**, 7863–7870.
25 J. Dulle, K. Thirunavukkarasu, M. C. Mittelmeijer-Hazeleger, D. V Andreeva, N. R. Shiju and G. Rothenberg, *Green Chem.*, 2013, **15**, 1238–1243.
26 A. Mariconda, M. Sirignano, C. Costabile and P. Longo, *Mol. Catal.*, 2020, **480**, 110570.
27 M.-T. Chen, B. Landers and O. Navarro, *Org. Biomol. Chem.*, 2012, **10**, 2206–2208.
28 I. Jesin and G. C. Nandi, *Eur. J. Org Chem.*, 2019, 2704–2720.
29 K. Dong, M. Liu and X. Xu, *Molecules*, 2022, **27**, 3088.
30 M. Turberg, K. J. Ardila-Fierro, C. Bolm and J. G. Hernández, *Angew. Chem., Int. Ed.*, 2018, **57**, 10718–10722.
31 S. I. Sampani, V. Zdorichenko, M. Danopoulou, M. C. Leech, K. Lam, A. Abdul-Sada, B. Cox, G. J. Tizzard, S. J. Coles, A. Tsipis and G. E. Kostakis, *Dalton Trans.*, 2020, **49**, 289–299.
32 J. Devonport, L. Sully, A. K. Boudalis, S. Hassell-Hart, M. C. Leech, K. Lam, A. Abdul-Sada, G. J. Tizzard, S. J. Coles, J. Spencer, A. Vargas and G. E. Kostakis, *JACS Au*, 2021, **1**, 1937–1948.
33 M. Ferguson, N. Giri, X. Huang, D. Apperley and S. L. James, *Green Chem.*, 2014, **16**, 1374–1382.
34 H. Katouah, A. M. Hameed, A. Alharbi, F. Alkhatib, R. Shah, S. Alzahrani, R. Zaky and N. M. El-Metwaly, *ChemistrySelect*, 2020, **5**, 10256–10268.
35 L. Leoni, A. Carletta, L. Fusaro, J. Dubois, N. A. Tumanov, C. Aprile, J. Wouters and A. D. Cort, *Molecules*, 2019, **24**, 2314.
36 V. K. Singh, A. Chamberlain-Clay, H. C. Ong, F. León, G. Hum, M. Y. Par, P. Daley-Dee and F. Garciá, *ACS Sustain. Chem. Eng.*, 2021, **9**, 1152–1160.
37 S. Zuo, S. Zheng, J. Liu and A. Zuo, *Beilstein J. Org. Chem.*, 2022, **18**, 1416–1423.
38 M. S. Maru, S. Barroso, P. Adão, L. G. Alves and A. M. Martins, *J. Organomet. Chem.*, 2018, **870**, 136–144.
39 W. Tan, J. Gao, J. Guan, X. Bi, Y. Tang, C. Zheng, T. Yan and C. Zhang, *J. Mol. Struct.*, 2022, **1269**, 133868.
40 I. Caretti, E. Carter, I. A. Fallis, D. M. Murphy and S. Van Doorslaer, *Phys. Chem. Chem. Phys.*, 2011, **13**, 20427–20434.
41 D. M. Murphy, I. Caretti, E. Carter, I. A. Fallis, M. C. Göbel, J. Landon, S. Van Doorslaer and D. J. Willock, *Inorg. Chem.*, 2011, **50**, 6944–6955.
42 S. Zamani, E. Carter, D. M. Murphy and S. Van Doorslaer, *Dalton Trans.*, 2012, **41**, 6861–6870.
43 S. Bunce, R. J. Cross, L. J. Farrugia, S. Kunchandy, L. L. Meason, K. W. Muir, M. O'Donnell, R. D. Peacock, D. Stirling and S. J. Teat, *Polyhedron*, 1998, **17**, 4179–4187.
44 A. Sharma, K. Mejia, H. Ueno, W. Zhou and L. Chiang, *Inorg. Chim. Acta*, 2022, **542**, 121106.
45 L. J. Zhu, D. H. Si, F. X. Ma, M. J. Sun, T. Zhang and R. Cao, *ACS Catal.*, 2023, **13**, 5114–5121.
46 D. Seidel, *Org. Chem. Front.*, 2014, **1**, 426–429.
47 D. Das, A. X. Sun and D. Seidel, *Angew. Chem., Int. Ed.*, 2013, **52**, 3765–3769.
48 *ICH, ICH Official web site: ICH*, **https://www.ich.org/page/quality-guidelines**, accessed 13 June 2023.
49 S. J. Coles and P. A. Gale, *Chem. Sci.*, 2012, **3**, 683–689.